

# Development of Textile-based Pressure Sensor and Its Application

Seung Ju Lim, Jong Hyuk Bae, Sung Jin Jang, Jee Young Lim, and Jae Hoon Ko\*

*Smart Textiles R&D Group, Korea Institute of Industrial Technology (KITECH), Ansan 15588, Korea*

(Received September 4, 2018; Revised October 2, 2018; Accepted October 4, 2018)

**Abstract:** Smart textile industries have been rapidly developed and are being studied for home care system. Particularly, the healthcare field has been highlighted in the smart device industries due to an increasingly ageing society, and pressure sensors can be utilized in various elderly healthcare products such as flooring and mattress because they can obtain a variety of pressure information in a large-area at indoor without infringing privacy. In this study, the novel type of conductive textile was fabricated using vapor phase polymerization (VPP) of poly(3,4-ethylenedioxythiophene) (PEDOT) to apply a textile to the pressure sensing device. The morphology of the PEDOT-coated conductive textile was observed through the field emission scanning electron microscope (FE-SEM). Moreover, the resistance was confirmed to be adjustable to various resistance ranges depending on the concentration of the oxidant solution and polymerization conditions and measured using 4-probe system. The 3-layered 81-points textile-based pressure sensor was fabricated using the PEDOT-coated conductive textile prepared herein. The visualized system by Matlab was developed to evaluate the sensitivity, multi-pressure recognition, and position tracking. In addition, the developed system can record the data so as to track the moving pressure and detect the event considered to be an emergency. Finally, we confirmed the possibility that PEDOT-coated conductive textiles could be utilized by pressure sensors.

**Keywords:** Smart textile, Textile pressure sensor, PEDOT, Vapor phase polymerization, Home care system

## Introduction

In recent years, various studies have been conducted on smart textiles that are combined with IT, NT, and BT. Smart textiles are being studied for home and health-related products [1]. The areas of application are expanding continuously, owing to the increase in the number of one-person (aged) households [2]. According to the World Health and Aging Report [3-5], elderly population (aged 65 or older) accounted for 8 % of the entire population in 2010, and the number of elderly individuals living alone is increasing rapidly [6]. Due to such an aging trend, the medical burden on the elderly population has been increasing. Indoor fall injuries are the most common cause requiring medical attention. Accidental falls are highly likely to cause cerebral hemorrhage [7]. Often, this may not be detected at an early stage for an elderly person living alone, resulting in severe consequences [8]. Therefore, it is necessary to develop a system that can notify a caretaker who is responsible for the elderly person's medical needs by using the relevant location information [9-11].

To identify the location information in residential settings, various methods have been attempted by using sensors. Such sensors include vision-based sensors [12,13], infrared sensors [14], acceleration sensors [15,16], and pressure sensors. Recent studies have further investigated the use of wireless communication-based (Zigbee, Bluetooth, RF, Wi-Fi) positioning technology to obtain the location information of indoor users [17-20]. Although, the infrared sensor is simple and inexpensive, it is difficult to perform measurements in places with sunlight exposure. Acceleration sensors and

wireless communication methods can be used to obtain the measurements by simple setups, which do not require installation of separate equipment indoors. However, these sensors are disadvantageous in a sense that the users are required to carry additional devices that would allow the measurements. Vision-based sensors are easy to install, requiring no additional equipment. Despite these advantages, privacy issues arising from continuous monitoring throughout the day still need to be addressed [21,22]. Pressure sensors have advantages, as they do not require any additional equipment to be carried individually. These sensors are capable of obtaining the user's location information without infringing the privacy.

Textile-based pressure sensors are flexible and stretchable. These sensors can be easily customized to fit different indoor structures. Furthermore, these textile-based pressure sensors can be utilized in a large-area positioning system by installing them on the floor. Such sensors are classified into piezoelectric, capacitive, and piezoresistive sensors, according to the underlying method of measurement. Among these sensor types, the piezoresistive sensor, which has a simple circuit configuration, can be used to perform dynamic/static pressure measurements. The piezoresistive sensor is not affected by the noise frequency commonly generated in a home environment. Due to these favorable attributes, the piezoresistive sensor is considered to be suitable for indoor applications.

To apply the textile to a pressure sensor, the textile must exhibit conductivity, and methods of providing conductivity to the textile have been widely researched [23-25]. In this study, vapor phase polymerization (VPP) was selected among the several methods for imparting conductivity to the textile. VPP is appropriate to impart conductivity into the

\*Corresponding author: ellafiz@kitech.re.kr

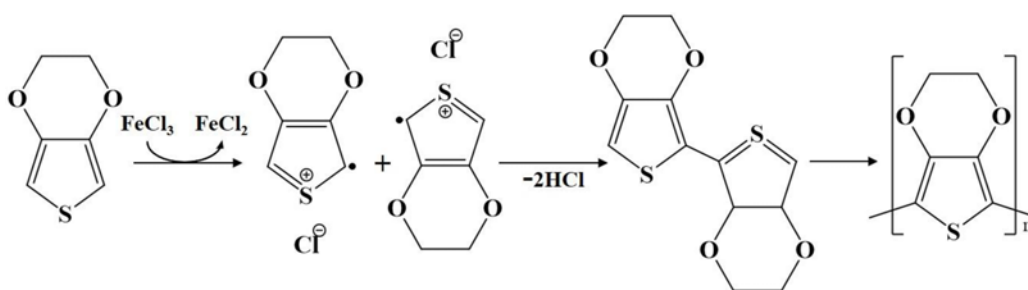


**Figure 1.** Vapor phase polymerization of PEDOT.

textile because a uniform thin film of nanoparticles is formed [26,27].

Polypyrrole (PPy) and poly(3,4-ethylenedioxythiophene) (PEDOT) are mainly used for VPP of textile materials; these are well-known conductive polymers that involve a simple fabrication process and exhibit excellent electrical properties. Due to the relatively high polymerization rate of PPy, it is difficult to control its conductivity [28]. However, because PEDOT has a slower reaction rate than PPy, PEDOT can be coated uniformly. As a result, this can be used to fabricate conductive textiles by controlling the conductivity using polymerization time control. Figure 1 shows the reaction scheme of PEDOT produced through VPP from EDOT.

Previous studies (such as [29]) have developed textile-type multi-pressure sensors by using PEDOT-coated conductive textile. Such a textile-based pressure sensor, which is a piezoresistive sensor, is composed of three layers. This type of sensor has a high sensitivity to pressure variation as small as 10 g. It measures the variation of resistance according to the pressure level at the time of application of pressure. However, to extract the position information, a position tracking system is needed that can utilize the conductive textile having a uniform resistance, and can store the received pressure information through the sensors.

Our study have developed a pressure-sensing system with a multi-layered structure. It serves as a prototype for use in large-area textile-based position tracking pressure-sensor system. This study applies a technically advanced VPP

method to fabricate a uniform conductive textile with no conductive gaps on both sides of the textile. We analyze the morphology and sheet resistance of the conductive textiles obtained through a FE-SEM (SU8010, HITACHI) and a 4-probe system (CMT-100S, Advanced Instrument Technology). We fabricated a textile-based pressure sensor by using PEDOT-coated conductive textile and constructed a system capable of tracking the position by utilizing the pressure information received from the sensors.

## Experimental

### Materials

Microfiber fabric (Welcron, Nylon/polyester splitting yarn) is used as the base to fabricate the conductive polymer thin-film coating fabric. This is used as the second layer (middle layer) of the multi-layer pressure sensor. In addition to EDOT (Sigma-Aldrich), which is used as a monomer of the conductive polymer, and  $\text{FeCl}_3$  (III) (Sigma-Aldrich) is used as an oxidizing agent in VPP. Reagents such as methyl alcohol (Duksan Laboratory, MeOH), and ethyl alcohol (Duksan Laboratory, EtOH) were also used. Materials and reagents used in this study were not purified further. A highly conductive fabric is used as an electrode for the first layer. Similarly, the third layer of the multi-layer pressure sensor also used a conductive fabric. These were sourced out to Solueta Co. Ltd., such that a PET fabric was plated with a nickel thin-film to impart resistances of several tens of ohms.

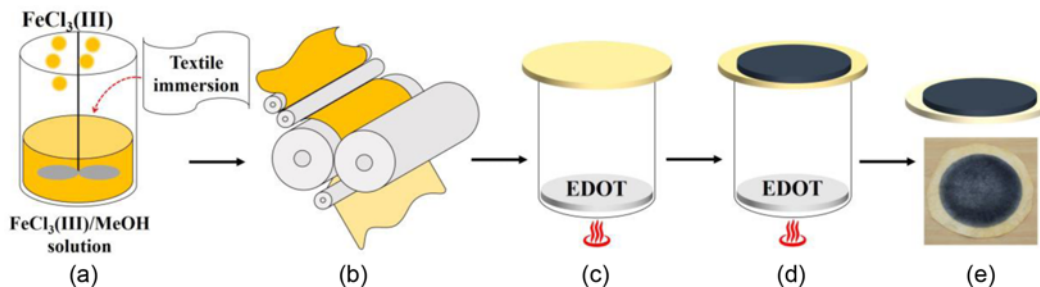


**Figure 2.** The process of VPP; (a) textile immersion into oxidizing solution, (b) mangling, (c, d) polymerization, and (e) PEDOT-coated conductive textile.

### Fabrication of Conductive Textile by VPP

The fabrication of conductive polymer thin-films through VPP requires the following processes (see Figure 2): preparation of oxidizing solution, substrate (textile) immersion, mangling, polymerization, washing, and drying [30].

The oxidizing solution was prepared by dissolving  $\text{FeCl}_3$  (III), an oxidizing agent, into MeOH, and by stirring it for a sufficient time. The concentration of the prepared oxidizing solution was optimized from 15 % to 20 % as suggested in the literature [31], and the optimum concentration for this research was selected as 20 % through preliminary experiments. The microfiber fabric was cut into appropriate sizes, and immersed into the prepared oxidizing agent solution for 30 min. This was mangled at a pick-up rate of 100 % and a mangle pressure of 0.05 MPa. This allowed the oxidizing solution to uniformly distribute throughout the textile. Typically, the reaction temperature of VPP for PEDOT is known to be in the range of 50–80 °C [30–32]. It was confirmed through preliminary experiments that the optimum reaction temperature was 60 °C in the polymerization reaction system used in this experiment. The EDOT (100 mg), which is a monomer of the conductive polymer, was placed into the reaction tank, and the temperature was elevated to 60 °C to generate sufficient monomer vapor in the reaction vessel. Subsequently, VPP reaction was performed by placing the oxidizing solution-immersed fabric on the top of the reaction tank. VPP was performed on both sides of the textile to fabricate a uniform conductive layer with no conductive gaps on either side. After the reaction was completed, the sample was washed and dried to fabricate a conductive PEDOT thin-film-coated textile. Optimum reaction conditions were established by varying the concentration of the oxidizing solution as well as the amount of EDOT in the reaction tank, and the values were as follow: 20 %  $\text{FeCl}_3$  (III)/MeOH solution, and 100 mg of EDOT. Once the

conditions were suitable, the experiment was conducted with the reaction time as variable to determine the optimal reaction time.

### Textile Pressure Sensing System

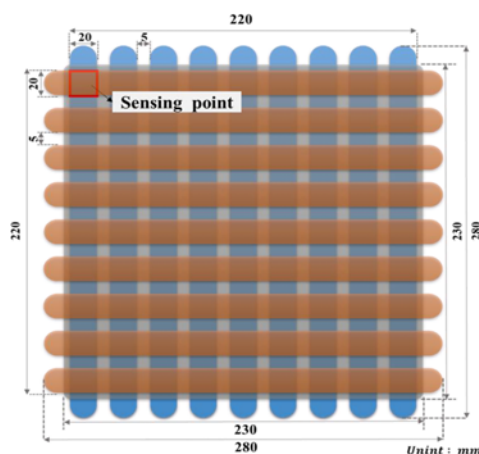
Typically, a textile-based piezoresistive sensor is composed of a multi-layer structure. A multi-layer structure is most commonly used due to its ease of implementation as well as mass-manufacturability [33]. Figure 3 shows a textile sensor composed of multi-layer conductive fabric developed through this work.

We developed the textile-based piezoresistive sensor as a prototype, which had a scale of 1:15 (actual flooring with 300 mm×300 mm). The sensor is fabricated with the dimension of 280 mm×280 mm. This includes the electrode, and consists 81 sensing points (in nine rows and nine columns). Because the sensing points are created by intersecting the top and bottom layers, each sensing point has a size of 20 mm×20 mm (line width of 20 mm).

Each line in the top and bottom layers are 20 mm and 280 mm in width and length, respectively. Furthermore, a nickel-plated fabric was applied to the outer layer (top and bottom layers) for us as an electrode. This has a lower resistance (0.6 ohm/sq) than the middle layer.

The middle layer has a dimension of 230 mm×230 mm (width by length), as well as a thickness of 0.65 mm. The thickness of the middle layer implies the length ( $l$ ) between the top and bottom. The thickness of the textile decreases as the applied vertical pressure on the textile increases. The resistance is given as  $R = \rho l / A$ . Since the resistance is proportional to the length, the resistance decreases with thickness.

One disadvantage of the textile-based sensors is that each layer is composed entirely of textiles. When the pressure is applied to the outside layer, the conductivity may be lost due



(a)



(b)

**Figure 3.** Textile-based pressure sensor; (a) structure diagram and (b) prototype.

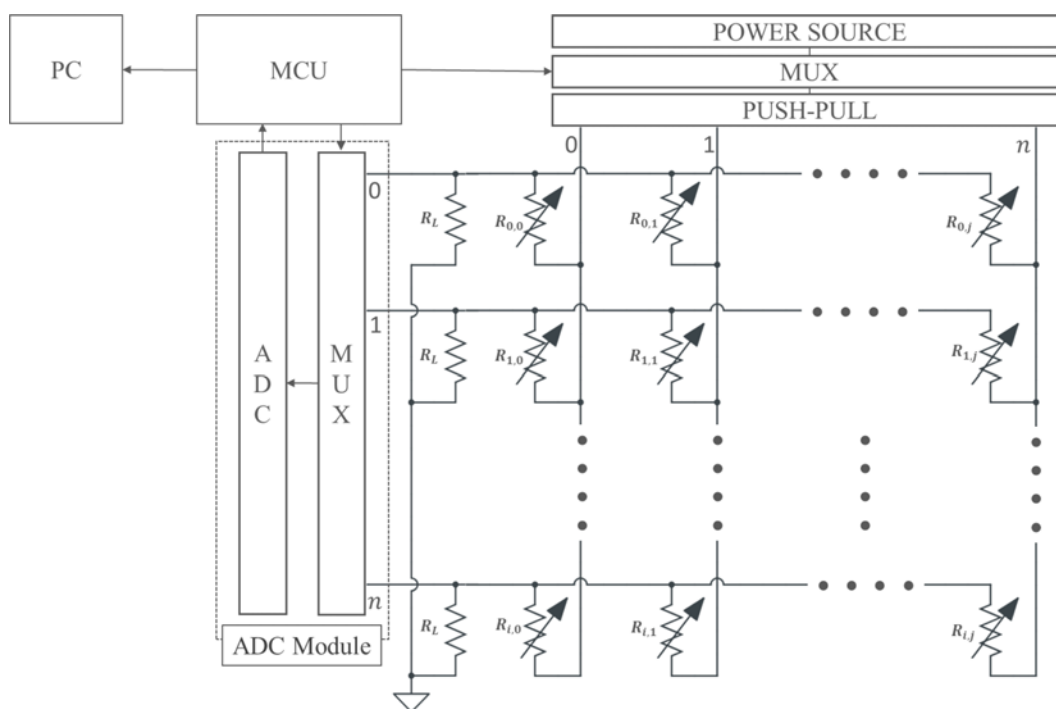


**Figure 4.** System architecture configuration of the textile-based pressure sensor.

to abrasion. The resistance of the conductive textile could vary due to moisture, thereby degrading the reliability of the measurements. To overcome these shortcomings, a protective film was covered on the surface of the sensors to minimize the conductivity degradation due to abrasion and moisture. Furthermore, when the textile sensor is not installed to a given fixture, slipping could occur due to pressure [33]. To prevent this slipping, the textile sensor was fixed onto the electrode of the PCB plate. The electrode with the fixed outside layer is connected to the ADC port of a micro controller.

Since the sensor has 81 sensing points, the sensor requires a large number of ADC ports. As the number of ADC ports increases, the unit price of the microcontroller becomes higher. Therefore, it is necessary to design a circuit that can minimize the number of ADC ports of MCU for pressure sensing. The designed circuit is shown in Figure 4.

To measure the variation in resistance caused by pressure, Kirchhoff's voltage law is applied. Here, a load resistor  $R_L$  and a sensing point resistance  $R_{ij}$  are used. The voltage across  $R_L$  is measured with  $R_L$  having a resistance value similar to  $R_{ij}$ , which is connected in series. The voltage across  $R_L$  varies according to the voltage drop/rise across  $R_{ij}$  which varies according to the pressure. The voltage is measured at the ADC port according to the following formula:

$$V_{ADC} = \frac{R_L}{R_L + R_{i,j}} V_{in}, \text{ where } i = 0, 1, \dots, n, j = 0, 1, \dots, n$$

The process of applying voltage to the system and reading the variation in resistance is performed sequentially. First, the MCU selects the channels of the MUX connected to the push-pull circuit from 0 to  $j$  sequentially, and the power source is applied to the selected column. If the 0th column is selected, the MCU selects the channels of the MUX connected to the ADC port from 0 to  $i$  sequentially, and measures the voltage across each  $R_L$ . Repeating this process up to the  $j$ th column, one can measure the resistance variations for all the sensing points from  $R_{0,0}$  to  $R_{i,j}$ .

Since the developed textile-based sensor is a prototype intended for application in indoor floor materials, it is designed to measure the resistance variation of a total of 81 sensing points in real-time. Furthermore, to track the movement of an elderly person in real-time, it is necessary to obtain the speed of walking.

An elderly person (aged 60 years and older) would walk at a step frequency of 1.4 Hz for slow walking, 1.7 Hz for normal walking and 1.9 Hz for fast walking [34]. The data sampling rate of the sensing system was determined to be approximately 10 Hz, considering frequent movements in a small radius (organizing things, cleaning, exercising, and other household activities). To obtain higher resolution measurements, the 16-bit ADC was used.

PJRC Teeny 3.2 was used as the microcontroller of the sensing system. For this microprocessor, 4.4  $\mu$ s is required to execute 1 byte, and the reading time of 81 sensing points is approximately 1.8 ms. This corresponds to a rate at which

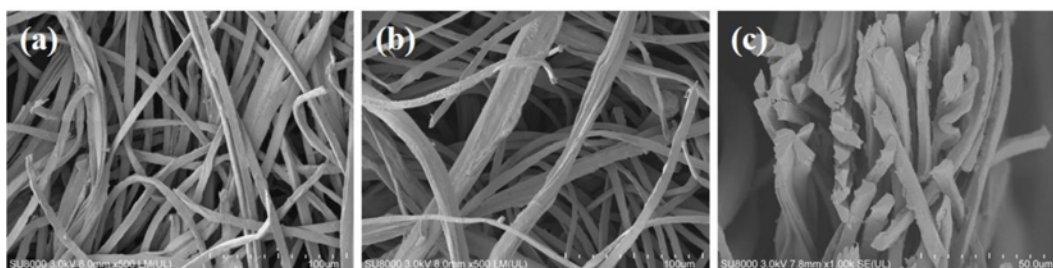


**Figure 5.** FE-SEM images of PEDOT-coated conductive textile fabricated from 2 hours VPP process for both sides; (a, b) both sides and (c) inner surface.

all the sensing points can be measured approximately 500 times.

## Results and Discussion

### Analysis of PEDOT-coated Conductive Textile

The morphology of the PEDOT-coated conductive textile prepared by VPP was analyzed by using FE-SEM. Because the oxidizing solution was uniformly applied to the textile through mangling during the VPP process, which was performed on both sides of the textile, PEDOT was formed uniformly on the surfaces of both sides of the textile. The results, which were fabricated from 2 hours VPP for both sides of the textile, are shown in Figure 5.

The conduction performance of PEDOT, which is a product of VPP, is influenced by the concentration of the oxidizing solution ( $\text{FeCl}_3(\text{III})/\text{MeOH}$ ) where the textile was immersed. This also depends on the amount of EDOT as a reactant during the polymerization reaction. We relied on the results of the previous studies, to establish the optimal reaction conditions for our experiments. The resistivity was evaluated for an oxidizing solution concentration of 20 %

and EDOT monomer amount of 100 mg. This was considered as the optimum reaction condition, based on the results in previous reports. However, it was observed that there is a resistance gap between the reaction surface and the back surface because the VPP process was applied only to one side of the textile. Table 1 shows the measured average resistance values, and it indicated the differences of average resistance between both sides. To fabricate a prototype of piezoelectric sensor capable of position tracking, and also scalable to large areas, there should ideally be no (or very small value of) resistance gaps between the two sides of the conductive textile. To achieve suitable value of the resistance and decrease differences of resistance between the two sides, the VPP process was applied on both sides of textile over time, and the results are shown in Table 2.

The average resistance value of the PEDOT-coated conductive textile according to the polymerization reaction time evidently decreased as the reaction time increased. After a six-hour reaction for 1 side VPP, the change was noticeably reduced while there was a resistance gap between the reaction side and the opposite side [29]. However, when the VPP was applied to both sides of the textile, the resistance was similar to that of the existing results (with two-hour reaction for each side), and the resistance difference between the two sides was found to be very small. Thus, the conductive textile applied in the second layer of a multi-layered pressure sensor that would be capable of position tracking was selected as: PEDOT-coated conductive textile fabricated with 20 % oxidizing solution, and 100 mg of EDOT that had undergone a two-hour VPP on each side.

To confirm the applicability of the selected conductive textile as a pressure sensor, the resistance change rate according to the weight was measured by using a standard weight, as shown in Figure 6.

The standard weight used in this measurement varies in the contact area with the sensor according to the weights. Thus, to accurately measure the pressure applied to the sensor, the standard weight was converted to pressure-per-unit-area, which would allow determination of the rate of resistance change of the sensor. The standard weights (10, 20, 50, 100, and 200 g) were converted into the pressure-per-unit-area to measure the resistances at 1.27, 1.51, 1.96, 2.63, and

**Table 1.** Average values of resistance between the two sides (1 side VPP)

| Reaction time | Average resistance ( $\text{k}\Omega/\text{sq}$ ) |               |
|---------------|---|---------------|
|               | Reaction side                                     | Opposite side |
| 1 hour        | N/D   |               |
| 2 hours       | 5.05  | 9.58          |
| 3 hours       | 3.68  | 6.36          |
| 6 hours       | 0.37  | 1.41          |

**Table 2.** Average values of resistance between the two sides (2 sides VPP)

| Reaction time<br>(each side) | Average resistance ( $\text{k}\Omega/\text{sq}$ ) |               |
|------------------------------|---|---------------|
|                              | One side  | Opposite side |
| 1 hour                       | N/D   |               |
| 2 hours                      | 3.85  | 4.29          |
| 3 hours                      | 1.05  | 5.48          |



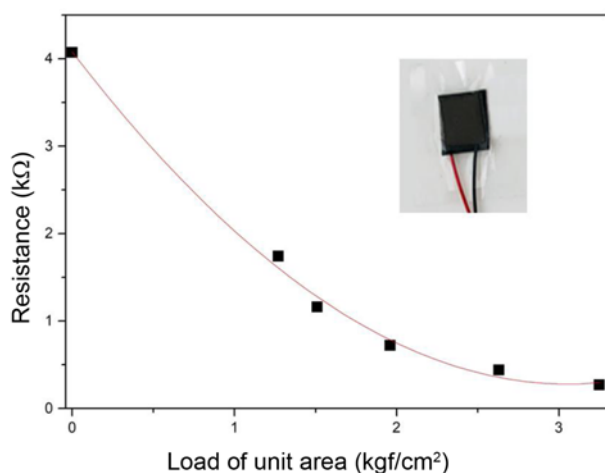


**Figure 6.** Resistance of textile-based pressure sensor according to change of the load.

3.25 kgf/cm<sup>2</sup>, respectively. After the selected conductive textile was formed into a single cell with a unit area size, the experiment was conducted. Applying 3.3 V, the load resistor  $R_L$  (4 kΩ) was connected in series with the sensor. The resistance value of the sensor was estimated through the voltage of the load resistance.

The results were 4.07, 1.74, 1.16, 0.72, 0.44, and 0.27 kΩ, respectively. It can be observed that as the pressure increases, the resistance decreases. This confirms that the fabricated conductive textile can be applied to the pressure sensor.

#### Evaluation of Textile-based Piezoresistive Sensor

A position tracking program using a textile-based piezoresistive sensor was implemented in Matlab 2018a. The performance of the textile-based pressure sensor is influenced by temperature and humidity. Furthermore, the number of sensors, the tension of the textile, and the

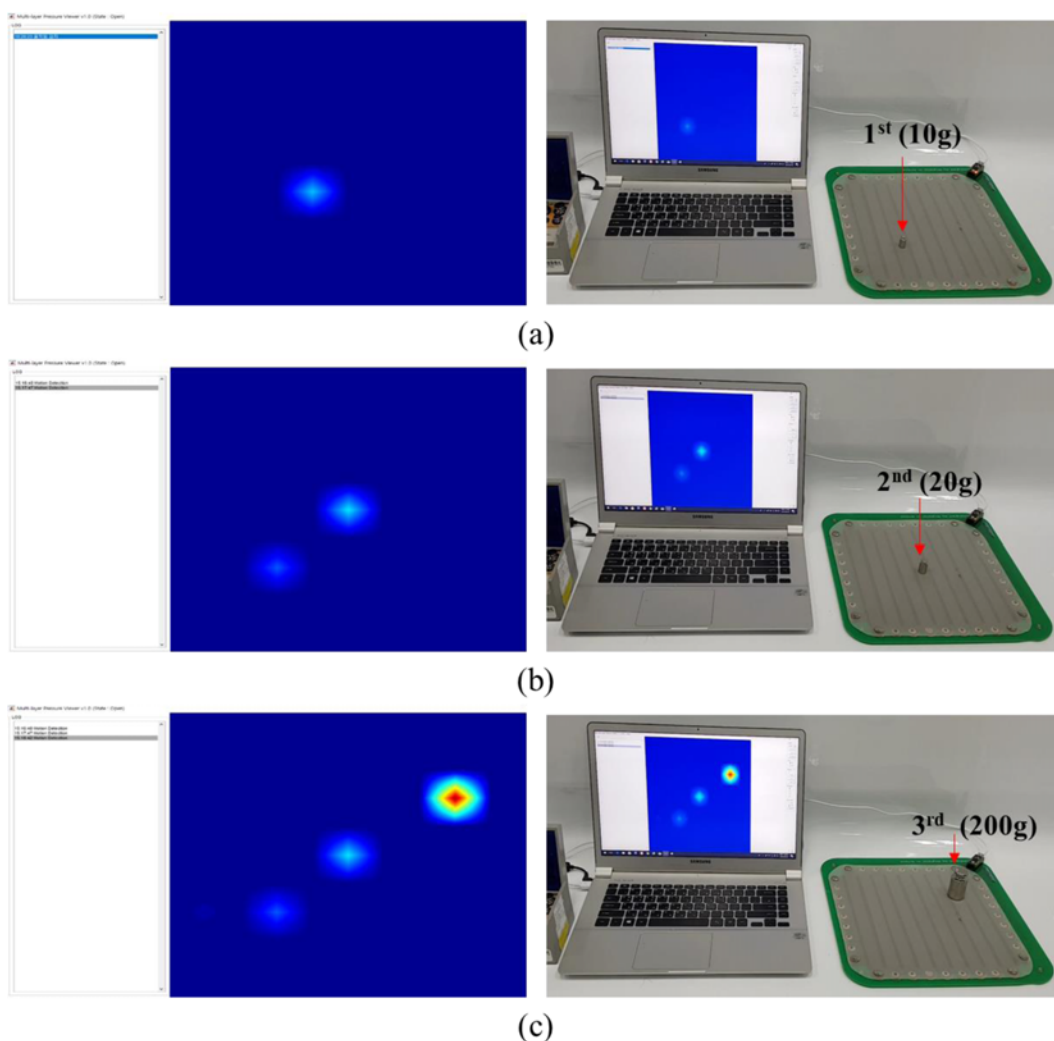


**Figure 7.** The visualization of textile-based pressure sensor using standard weight; (a) 10 g, (b) 20 g, and (c) 200 g.

unevenness of the conductivity could lead to resistance deviations at each sensing point. To overcome this drawback, the average value of the data acquired for 10 seconds after the start of the program was set as a reference value. The change in resistance from the reference resistance was further measured by applying pressure.

To confirm a real-time position tracking, the pressure was applied at various points as shown in Figure 7.

We conducted both tracking and measurement of rate of change pressure variations using the pressure sensor fabricated in this research. The pressure change rate was confirmed by identifying the color changes, which were observed by placing the standard weights on the sensing points. The pressure changes were measured by using different weights of 10 g, 20 g, and 200 g while varying the sensing points. These are shown in Figure 7(a), (b), and (c), in sequence. The position of the sensing point was changed. As shown in Figure 7(a) and 7(b), the sensitivity of the

pressure was visually distinguishable even with a 10 g weight difference. As shown in Figure 7(c), despite a pressure being applied to one sensing point (200 g) by using the pressure input in the past (Figure 7(a) and 7(b)), the current position and the past position could be visually identified using the position tracking system.

When the pressure sensor is applied as indoor flooring, the pressure of the furniture is regarded as a fixed pressure, and this pressure can interfere with the recognition of the urgent state of the elderly people. Therefore, the moving pressure (pressure on human movement) should be sensed separately from the fixed pressure and be able to be tracked in real time. A program that can track the user's movement in the presence of a fixed object is shown in Figure 8.

Figure 8 showed a system capable of tracking the pressure of a moving person in the presence of a fixed object. As shown in Figure 8(a) is virtual pressure tracking when there is only a moving person, Figure 8(b) is a virtual pressure

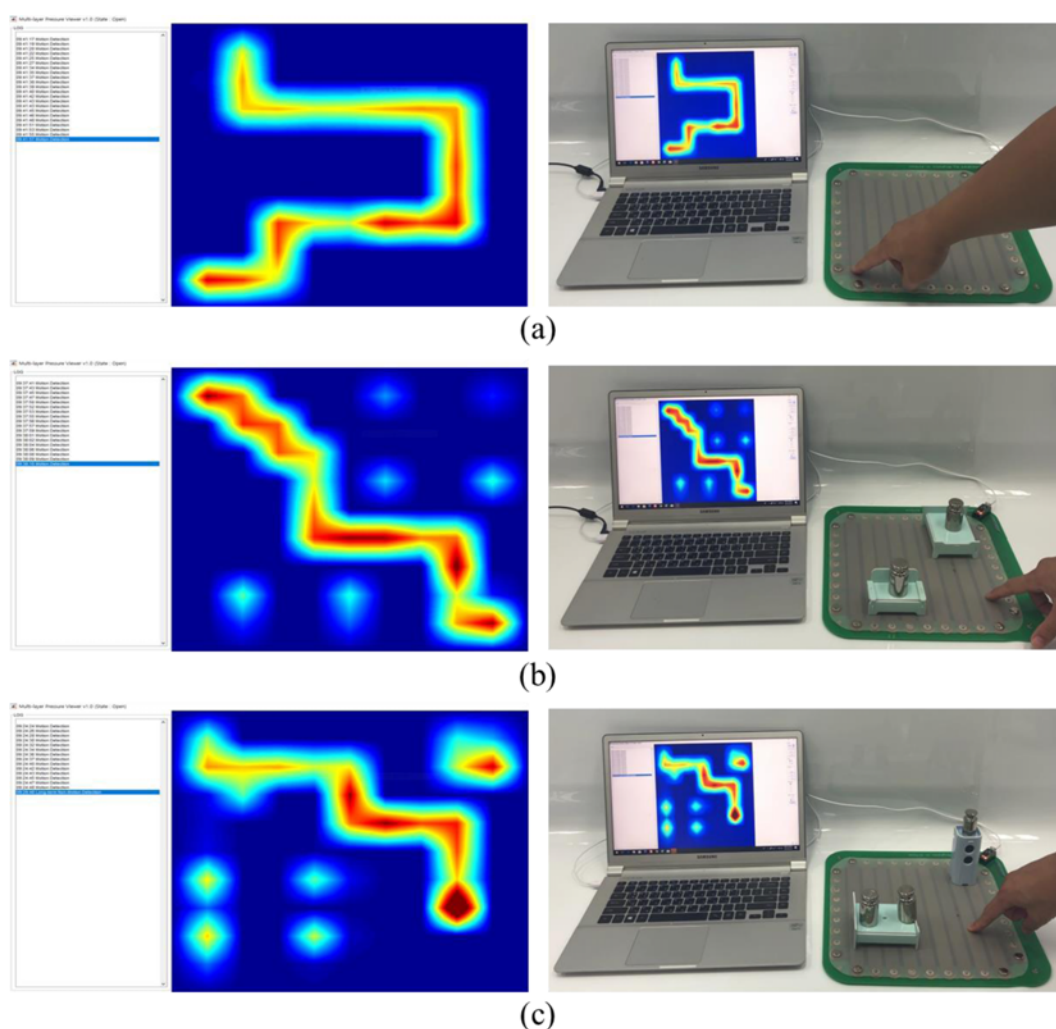


**Figure 8.** The visualization of textile-based pressure sensor; (a) only moving pressure, (b) moving pressure with fixed pressure, and (c) the event considered to an emergency.

tracking when a person moves in the presence of a fixed object, and Figure 8(c) is a simulation of detecting the dangerous situation of a person.

The pressure sensor developed in this study was able to simultaneously measure the moving pressure and the intensity of the pressure in real time. The system was able to separate the fixed pressure and accurately track only the moving pressure. When a new moving pressure is detected, the log window displays the message 'Motion detection' and the detection time is recorded. The system is also designed to detect dangerous situations if there is no change for a period of time (5 minutes) after the moving pressure is stopped. When a dangerous situation is detected, the log window displays the message 'Long-term non-motion detection' and the time of occurrence, recording the risk every 5 minutes.

As shown in Figure 8, the textile-based piezoresistive sensor developed in this study can measure the pressure change of each sensing point even when various fixed pressures are applied. This method can estimate the user's motion by detecting the moving pressure even when there is furniture across the room in a real-world environment. Since a large-area sensor can be easily formed on the entire floor using this sensor, accurate detection of the user's absolute position is possible.

## Conclusion

This work developed a PEDOT thin-film coating textile with improved conductivity and uniformity by using vapor phase polymerization. In addition, we developed a textile-based multi-layer pressure-sensing system capable of position tracking using the PEDOT thin-film coating textile. The developed textile-based multi-pressure sensing system not only enables multiple pressure measurements in real-time, but also enables position tracking through the stored information. The developed textile-based multi-pressure sensing system was implemented in Matlab 2018a. This study confirms the feasibility of fabricating a large-area textile-based pressure-sensing system through extensive experiments on sensor sensitivity, multi-recognition, and position tracking.

The sensor developed in this work can be configured for a large area. This can reduce the foreign sensation felt by the user due to the thickness of the sensor. It is possible to recognize the absolute position of the user by using a large-area sensor and by tracking the moving pressure in an indoor environment. As a result, the sensor can detect a sudden movement by an elderly person, alerting the caregivers of an emergency situation, such as falls or trips.

## Acknowledgements

This work was supported by the Korea Institute of

Industrial Technology (EO180016).

## References

1. M. Stoppa and A. Chiolerio, *Sensors*, **14**, 11957 (2014).
2. N. Singleton, R. Bumpstead, M. O'Brien, A. Lee, and H. Meltzer, *International Review of Psychiatry*, **15**, 65 (2009).
3. World Health Organization, "Global Health and Ageing", *World Health Organization*, Geneva, 2011.
4. Y. L. Hsu, P. H. Chou, H. C. Chang, S. L. Lin, S. C. Yang, H. Y. Su, C. C. Chang, Y. S. Cheng, and Y. C. Kuo, *Sensors*, **17**, 1631 (2017).
5. United-Nations, "World Population Prospects: The 2008 Revision", United Nations Publication, New York, 2018.
6. W. C. Mann, *IEEE Pervasive Computing*, **3**, 12 (2004).
7. World Health Organization, "Global Brief for World Health Day, World Health Organization, Geneva, 2012.
8. Z.P. Bian, J. Hou, L. P. Chau, and N. M. Thalmann, *IEEE J. Biomed. Health Inform.*, **19**, 430 (2015).
9. S. Consolvo, P. Roessler, B. E. Shelton, A. LaMarca, B. Schilit, and S. Bly, *IEEE Pervasive Computing*, **3**, 22 (2004).
10. E. D. Mynatt, A. S. Melenhorst, A. D. Fisk, and W. A. Rogers, *IEEE Pervasive Computing*, **3**, 36 (2004).
11. A. Sixsmith and N. Johnson, *IEEE Pervasive Computing*, **3**, 42 (2004).
12. A. Mulloni, D. Wagner, I. Barakonyi, and D. Schmalstieg, *IEEE Pervasive Computing*, **8**, 22 (2009).
13. M. Heikkila and M. Pietikainen, *The IEEE Transactions on Pattern Analysis and Machine Intelligence*, **28**, 657 (2006).
14. A. Sixsmith, N. Johnson, and R. Whatmore, *J. Phys. IV France*, **128**, 153 (2005).
15. E. Foxlin, *IEEE Computer Graphics and Applications*, **25**, 38 (2005).
16. S. W. Lee and K. Mase, *IEEE Pervasive Computing*, **1**, 24 (2002).
17. Z. Farid, R. Nordin, and M. Ismail, *Journal of Computer Networks and Communications*, **2013**, 1 (2013).
18. Y. Gu, A. Lo, and I. Niemegeers, *IEEE Communications Surveys and Tutorials*, **11**, 13 (2009).
19. S. Gezici, *Wireless Personal Communications*, **44**, 263 (2008).
20. M. B. Kjærsgaard, *Pervasive and Mobile Computing*, **7**, 31 (2011).
21. D. Stojanović and N. Stojanović, *Automatic Control and Robotics*, **31**, 57 (2014).
22. A. Khoshgozaran and C. Shahabi, *Int. J. Comput. Sci. Eng.*, **5**, 86 (2010).
23. A. Ali, V. Baheti, J. Militky, Z. Khan, and S. Q. Z. Gilani, *Fiber. Polym.*, **19**, 607 (2018).
24. S. Ghosh, S. Mondal, S. Ganguly, S. Remanan, N. Singha, and N. Ch. Das, *Fiber. Polym.*, **19**, 1064 (2018).
25. R. Navik, F. Shafiq, A. Khan, M. Datta, X. Peng, Md.



- Kamruzzaman, and Y. Cai, *Fiber. Polym.*, **18**, 1115 (2017).
26. M. Fabretto, K. Zuber, C. Hall, and P. Murphy, *Macromol. Rapid Commun.*, **29**, 1403 (2008).
27. J. Kim, D. Sohn, Y. Sung, and E. R. Kim, *Syn. Met.*, **132**, 309 (2003).
28. K. H. Hong, K. W. Oh, and T. J. Kang, *J. Appl. Polym. Sci.*, **97**, 1326 (2005).
29. S. J. Lim, J. H. Bae, J. Y. Lim, K. H. Park, S. J. Jang, and J. H. Ko, *The Korean Sensors Society*, **27**, 186 (2018).
30. A. Laforgue and L. Robitaille, *Macromolecules*, **43**, 4194 (2010).
31. M. Fabretto, K. Zuber, C. Hall, P. Murphy, and H. J. Griesser, *J. Mater. Chem.*, **19**, 7871 (2009).
32. T. Bashir, L. Fast, M. Skrifvars, and N. K. Persson, *J. Appl. Polym. Sci.*, **12**, 2954 (2012).
33. I. Baldoli, M. Maselli, F. Cecchi, and C. Laschi, *Smart Mater. Struct.*, **26**, 1 (2017).
34. J. E. Himann, D. A. Cunningham, P. A. Rechnitzer, and D. H. Paterson, *Med. Sci. Sports and Exercise*, **20**, 161 (1988).